

OPEN

Performance of composite mineral adsorbents for removing Cu, Cd, and Pb ions from polluted water

Woo-Ri Lim¹, Sung Wook Kim², Chang-Han Lee³, Eun-Kyeong Choi², Myoung Hak Oh⁴, Seung Nam Seo⁴, Heung-Jai Park⁵ & Se-Yeong Hamm¹

This study evaluated the efficiency of the removal of heavy metals from contaminated water via adsorption isotherm and kinetic experiments on two composite mineral adsorbents, CMA1 and CMA2. The developed CMA1 (zeolite with clinoptilolite of over 20 weight percent and feldspar of ~10 percent, with Portland cement) and CMA2 (zeolite with feldspar of over 15 weight percent and ~9 percent clinoptilolite, with Portland cement) were applied to remove Cu, Cd, and Pb ions. Based on the adsorption isotherm and kinetic experiments, the adsorbents CMA1 and CMA2 exhibited high removal efficiency for Cu, Cd, and Pb ions in solution compared to other adsorbents. In the adsorption kinetic experiment, CMA2 demonstrated better adsorption than CMA1 with the same initial concentration and reaction time, and Cu, Cd, and Pb ions almost reached equilibrium within 180 min for both CMA1 and CMA2. The results of the adsorption kinetic experiments with pseudo-first-order (PFO) and pseudo-second-order (PSO) models indicated that the PSO model was more suitable than the PFO model. Comparing the Langmuir and Freundlich adsorption isotherm models, the former showed a very slightly higher correlation coefficient (r^2) than the latter, indicating that the two models can both be applied to heavy metal solutions on a spherical monolayer surface with a weak heterogeneity of the surface. Additionally, the adsorbents CMA1 and CMA2 demonstrated different removal abilities depending on which heavy metals were used.

Substantial research has been conducted in the past 20 years on which materials are best for adsorbing heavy metals (Table 1). Garcia-Sánchez *et al.*¹ evaluated the heavy-metal adsorption capacity of clay minerals (sepiolite, palygorskite, and bentonite) from different mineral deposits with a reduction in metal mobility and bioavailability for remediation of polluted soils in the Guadiamar Valley. Erdem *et al.*² studied the adsorption behaviour of natural clinoptilolite with respect to Co, Cu, Zn, and Mn ions and found that the adsorption was dependent on charge density and hydrated ion diameter, showing great potential for natural clinoptilolite to remove cationic heavy metal species from industrial wastewater. Ok *et al.*³ studied a mixture of zeolite and Portland cement (ZeoAds) as a substitute for activated carbon and tested its efficiency for the removal of heavy metals from aqueous solutions for wastewater treatment. Park and Hwang⁴ used adsorption tests to evaluate feldspar porphyry as an adsorbent for heavy metals in natural water. Nguyen *et al.*⁵ determined the adsorption behaviours of Cd, Cu, Cr, Pb, and Zn individually and collectively on an Australian natural zeolite with an iron coating (ICZ). He *et al.*⁶ carried out isotherms and kinetics studies using a synthesized zeolite from fly ash to investigate the adsorption capacity of heavy metal ions (Pb, Cu, Cd, Ni, and Mn) in aqueous solutions. Taamneh and Sharadqah⁷ evaluated the use of natural Jordanian zeolite (NJ zeolite) as a practical adsorbent for removing Cd and Cu ions. Lee *et al.*⁸ evaluated the adsorption performance of valuable metal ions (Cu, Co, Mn, and Zn) using a synthesized zeolite (Z-C2) from fly ash.

Various researchers^{9–13} have characterized the chemical, surface, and ion-exchange properties of clinoptilolite. Zamzow *et al.*¹¹ studied the inorganic cation exchange capacity of clinoptilolite and the selectivity series as

¹Department of Geological Sciences, Pusan National University, 63beon-gil 2, Geumjeong-gu, Busan, 46241, Republic of Korea. ²GI Co., Ltd., 11, 1048beon-gil, Joongang-daero, Yeonje-gu, Busan, 47598, Republic of Korea.

³Department of Environmental Administration, Catholic University of Pusan, 57 Oryundae-ro, Geumjeong-gu, Busan, 46252, Republic of Korea. ⁴Coastal Disaster Prevention Research Center, Korea Institute of Ocean Science & Technology, 385, Haeyang-ro, Yeongdo-gu, Busan, 49111, Republic of Korea. ⁵Department of Environmental Engineering, Inje University, 197, Inje-ro, Gimhae, 50834, Republic of Korea. Correspondence and requests for materials should be addressed to S.-Y.H. (email: hsy@pusan.ac.kr)

Adsorbent materials	Absorbent dose to heavy metal solution (g/L)	Time (h)	Temp. (°C)	Adsorbed heavy metals (Maximum adsorption capacity, mg/g)								Authors	
				Cd	Co	Cu	Cr	Fe	Pb	Mn	Ni		Zn
Clays (sepiolites, palygorskites, and bentonite from different mineral deposits)	5	2	22	8.3		6.9						5.7	García-Sánchez <i>et al.</i> ¹
Clinoptilolite	20	5.5	30	9	14.4					4.2		8.8	Erdem <i>et al.</i> ²
Activated carbon	40	24	25	6.4		12.3			18.4			7.2	Ok <i>et al.</i> ³
ZeoAds (mixture of zeolite and Portland cement)	40	24	25	10.9		23.3			27			12.9	Ok <i>et al.</i> ³
ICZ (iron-coated zeolite)	1–25	24	25 ± 2	7.24		9.33	5.47		11.16			6.22	Nguyen <i>et al.</i> ⁵
Zeolite synthesized from coal fly ash	10	3	30	52.12		56.06			65.75	30.89	34.4		He <i>et al.</i> ⁶
NJ zeolite (natural Jordanian zeolite)	20	24	22	25.9		14.3							Taamneh and Sharadqah ⁴
Z-C2 (synthesized zeolite from fly ash)	1	4	30		77.7	94.7				57.7		51.1	Lee <i>et al.</i> ⁸

Table 1. Adsorption results of heavy metals by various adsorbent materials.

follows: $Pb^{2+} > Cd^{2+} > Cs^{+} > Cu^{2+} > Co^{2+} > Cr^{3+} > Zn^{2+} > Ni^{2+} > Hg^{2+}$. Jama and Yücel¹⁰ recognized a very high preference of clinoptilolite for ammonium ions over sodium and calcium ions but not over potassium ions. Mier *et al.*¹² identified the interactions of Pb^{2+} , Cd^{2+} , and Cr^{3+} competing for ion-exchange sites in natural clinoptilolite. Regarding the ion exchange of Pb^{2+} , Cu^{2+} , Fe^{3+} , and Cr^{3+} on natural clinoptilolite, Inglezakis *et al.*¹³ found that equilibrium is favourable for Pb^{2+} , unfavourable for Cu^{2+} , and of sigmoidal shape for Cr^{3+} and Fe^{3+} . Since commercial clinoptilolite is relatively costly, mixtures of zeolite and other less expensive organic and inorganic materials, such as cement, clays, and polymers, have been formulated for specific pollutants¹⁴.

Recently, functionalized adsorbents such as nanocomposite materials have been prepared for harmful heavy metal ions and organic compound adsorption and have been used for diverse applications^{15–23}. Moreover, natural mineral-modified adsorbents have the advantage that they can be applied not only to the aqueous phase but also to the soil phase^{24–29}. This study aimed to reveal the efficiency of the removal of heavy metals by applying modified natural minerals as adsorbents to contaminated groundwater. For this purpose, we evaluated the cation adsorption performance and adsorption equilibrium characteristics of the composite mineral adsorbents CMA1 (zeolite with clinoptilolite of over 20 weight percent and feldspar of ~10 percent, with Portland cement) and CMA2 (zeolite with feldspar of over 15 weight percent and ~9 percent of clinoptilolite, with Portland cement) through adsorption isotherms and kinetics. Specifically, we looked at how CMA1 and CMA2 performed in the removal of Cu, Cd, and Pb ions from polluted water.

Materials and Methods

Preparation and characterization of the adsorbents. The preparation procedure of the adsorbents CMA1 and CMA2 is illustrated in Fig. 1. All experiments were conducted in a 10-L polyethylene reactor equipped with a stirrer. To prepare the adsorbents CMA1 and CMA2, clinoptilolite-rich zeolite, slightly weathered feldspars showing a porous structure under a microscope, and normal Portland cement were prepared. Porous feldspar was prepared from weathered feldspar porphyry that was pulverized into 44- μ m particles after being heated at 480 °C for 20 min. For the CMA1 adsorbent, a mixture of clinoptilolite-rich zeolite (C) and Portland cement (PC) at a ratio of C:PC = 70:30 wt% was cured for 28 days after adding water and lightweight foam. Finally, the CMA1 adsorbent powder was made by crushing the cured specimen. For the CMA2 adsorbent, a mixture of clinoptilolite-rich zeolite (C), porous feldspar (PF), and Portland cement (PC) at a ratio of C:PF:PC = 40:30:30 wt% was cured for 28 days after adding water and lightweight foam. Eventually, the CMA2 adsorbent powder was produced by crushing the cured specimen.

Crystallization and chemical characterization were performed by X-ray diffraction (XRD, Philips X'Pert-MPD System). XRD patterns of the samples were scanned on a powder diffractometer with Cu K α radiation ($\lambda = 1.54$ Å) at a diffraction angle of 2θ in the range of 5–50° in 0.02° steps (3 s per step). The crystal morphologies of the samples were analysed by using scanning electron microscopy (SEM, Hitachi S-4200), with an accelerating voltage of 15 kV and a magnification of 20,000 times. The samples were coated with a thin layer of platinum and mounted on a copper slab using double-sided tape for the SEM analysis.

Methodology. Batch tests were performed for adsorption isotherm and adsorption kinetic experiments using the two adsorbents (CMA1 and CMA2) and standard heavy metal (Cu, Cd, and Pb ions) solutions for the different ion adsorption performance and adsorption equilibrium characteristics. The adsorption isotherm and kinetic experiments were conducted to determine the adsorption characteristics and adsorption rate, respectively, of the heavy metal ions. Fifty millilitres of Cu, Cd, and Pb ion solutions and 0.05 g of CMA1 and CMA2 were placed in a 50-mL conical centrifuge tube (Falcon, 352070) and stirred at 200 rpm using a horizontal shaker (Vision, VS-8480S). For the adsorption kinetic experiment, 0.05 g of the adsorbent was added and stirred with 50 mL of a 1,000 mg/L heavy metal solution, and the residual concentration was analysed at reaction times of 30, 60, 90, 120, 180, 360, and 480 min. For the adsorption isotherm experiment, 0.05 g of the adsorbent was added to 50 mL of 50–1,000 mg/L heavy metal solution with stirring, and the residual concentration was analysed after 24 h of reaction time. The pH change experiments were conducted with 1,000 mg/L Cu, Cd, and Pb ion solutions

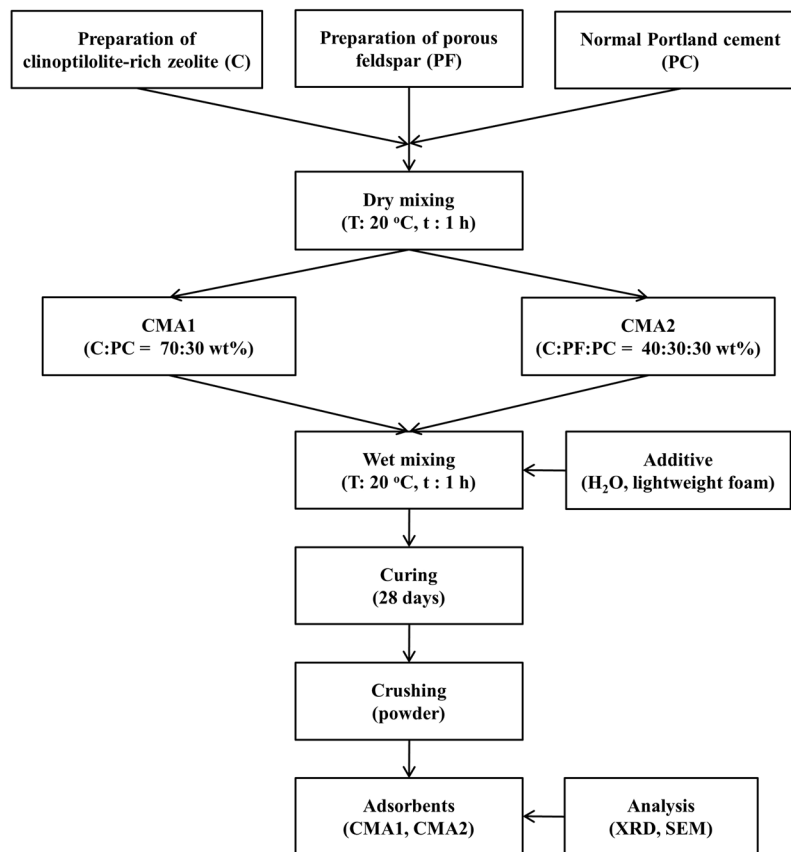


Figure 1. Procedure and analysis performed during preparation of the adsorbents CMA1 and CMA2.

at 25 °C. The initial pH in the solutions was adjusted to 3.0, 5.0, or 7.0 by adding 0.5 M HNO₃ or 0.5 M NaOH solution. The pH values were measured using a pH meter (Istek AJ-7724, Korea).

Samples were taken at regular intervals and centrifuged (Vision Scientific VS-5000i2, Korea) for 3 min at 3,000 rpm. After centrifugation, the supernatant was filtered, and the Cu, Cd, and Pb ion concentrations were analysed by using an atomic absorption spectrophotometer (Perkin Elmer AAnalyst 100, Germany).

Theory

Adsorption kinetics. The pseudo-first-order (PFO) rate equation for the adsorption kinetics of solutes from a liquid solution that was proposed by Lagergren³⁰ is:

$$\frac{dq}{dt} = k_1(q_e - q) \quad (1)$$

where q and q_e are the amounts of solute adsorbed (mg) per adsorbent (g) at any time and at equilibrium, respectively, and k_1 is the PFO rate constant of adsorption. Integrating Eq. (1) for the boundary conditions $t = 0$ to t and $q = 0$ to q gives:

$$\ln \frac{(q_e - q)}{q_e} = -k_1 t \quad (2)$$

The pseudo-second-order (PSO) rate equation for the adsorption kinetics of solutes from a liquid solution proposed by Ho and McKay³¹ is:

$$\frac{dq}{dt} = k_2(q_e - q)^2 \quad (3)$$

The integration of Eq. (3) for the boundary conditions $t = 0$ to t and $q = 0$ to q gives:

$$\frac{1}{q_e - q} = \frac{1}{q_e} + k_2 t \quad (4)$$

where k_2 is the PSO rate constant of adsorption. A linear equation can then be obtained from Eq. (4):

$$\frac{t}{q} = \frac{1}{k_2 q_e^2} + \frac{1}{q_e} t \quad (5)$$

The plot of t/q versus t gives a straight line with a slope of $1/q_e$ and an intercept of $1/k_2 q_e^2$, and then q_e and k_2 can be evaluated from the slope and intercept, respectively.

Adsorption isotherms. According to the formula by Vanderborght and Van Grieken³², Q , the solute adsorbed (mg) per adsorbent (g), is

$$Q = \frac{V(C_i - C_e)}{W} \quad (6)$$

where V is the volume of the adsorbate (L), C_i is the initial concentration of adsorbate (mg/L), C_e is the concentration of the adsorbate after adsorption (mg/L), and W is the weight of the adsorbent (g). The experimentally derived isotherm can be fitted into the Langmuir³³ and Freundlich³⁴ adsorption isotherms, which represent, respectively, uniform adsorption energy onto the surface with no transmigration of adsorbate in the plane of the surface and the adsorption on a heterogeneous surface. The Langmuir adsorption isotherm is valid for monolayer adsorption onto a surface that contains a finite number of identical sites. The removal efficiency expressed as the percent of sorption is:

$$\% \text{ Sorption} = \frac{C_i - C_e}{C_i} \times 100 \quad (7)$$

According to Langmuir, the amount adsorbed, Q_e (mg/g), is defined as:

$$Q_e = \frac{Q_m K_L C_e}{1 + K_L C_e} \quad (8)$$

where C_e is the equilibrium concentration of the adsorbate (mg/L), Q_m is the Langmuir constant related to the maximum monolayer adsorption capacity (mg/g), and K_L is the Langmuir isotherm coefficient related to the affinity of the sorbate for the binding sites. Equation (8) can be re-arranged into a linear form:

$$\frac{1}{Q_e} = \frac{1}{Q_m} + \frac{1}{Q_m K_L C_e} \quad (9)$$

Using the Freundlich equation, the amount adsorbed, Q_e (mg/g), is:

$$Q_e = K_F C_e^{1/n} \quad (10)$$

Thus, linearizing Eq. (10),

$$\ln Q_e = \ln K_F + \frac{1}{n} \ln C_e \quad (11)$$

where K_F is the Freundlich isotherm coefficient or an approximate indicator of the adsorption capacity (mg/g), $1/n$ is a function of the strength of the adsorption in the adsorption process, and n is the adsorption intensity³⁵. A value of $n = 1$ indicates that the partition between the two phases is independent of the concentration, $n > 1$ indicates normal adsorption, and $n < 1$ indicates cooperative adsorption³⁶. A value of $1 < n < 10$ demonstrates a favourable sorption process³⁷. The constant change of K_F and n with an increase in temperature reflects the empirical observation that the quantity adsorbed rises more slowly, such that higher pressures are required to saturate the surface. For the determination of K_F and n by data fitting, linear regression is generally used to determine the parameters of the kinetic and isotherm models³⁸. The linear least-squares method and linearly transformed equations have been widely applied to correlate sorption data, where the smaller the $1/n$ (or heterogeneity parameter), the greater the expected heterogeneity.

Results

Characterization of the adsorbents. The composite mineral adsorbents, CMA1 and CMA2, are composed of clinoptilolite, feldspars, and Portland cement. XRD analysis showed that CMA1 and CMA2 consisted of albite, calcite, dachiardite, clinoptilolite, and mordenite (Fig. 2). Feldspar is reported to have a heavy metal adsorption capacity^{39–41}. Clinoptilolite, with the chemical formula of $(\text{Na,K})_{64}\text{Al}_6\text{Si}_{30}\text{O}_{72} \cdot n\text{H}_2\text{O}$, one of most abundant natural zeolites, is found in sedimentary rocks of volcanic origin and occurs with silicate minerals such as feldspar, quartz, other zeolites (members of the tectosilicates subclass), clays (members of the phyllosilicates subclass), and volcanic glass⁴². Clinoptilolite, along with heulandite and mordenite, has a high cation capacity⁴³. Its tabular morphology shows an open reticular formation with easy access, formed by open channels of 8- to 10-membered rings. Feldspars, anhydrous aluminosilicates composed of potassium, sodium, and calcium, are structured by silicon and aluminium occupying the centres of the tetrahedrals of SiO_4 and AlO_4 . These tetrahedrals are linked to other tetrahedrals at each corner, forming a 3-D, negatively charged framework. Potassium, sodium, and calcium within the voids of the structure can be exchanged with other cations. Portland cement is a very common solidification and stabilization material and is used as a supplement to clinoptilolite for adsorption

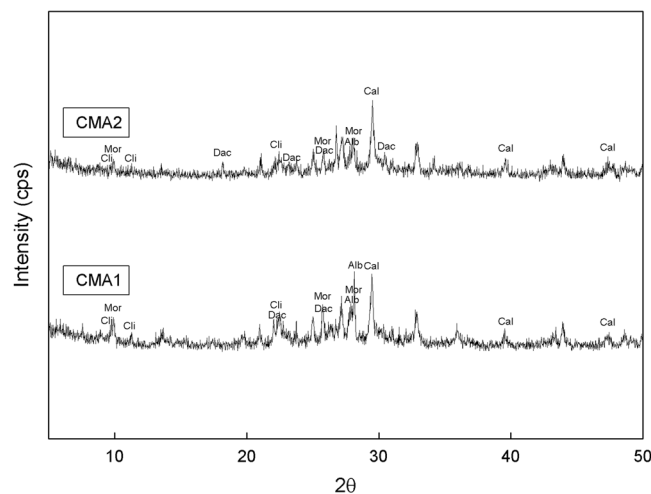


Figure 2. XRD peaks of the composite mineral adsorbents CMA1 and CMA2. Albite (Alb), Calcite (Cal), Dachiardite (Dac), Clinoptilolite (Cli), and Mordenite (Mor) have been identified.

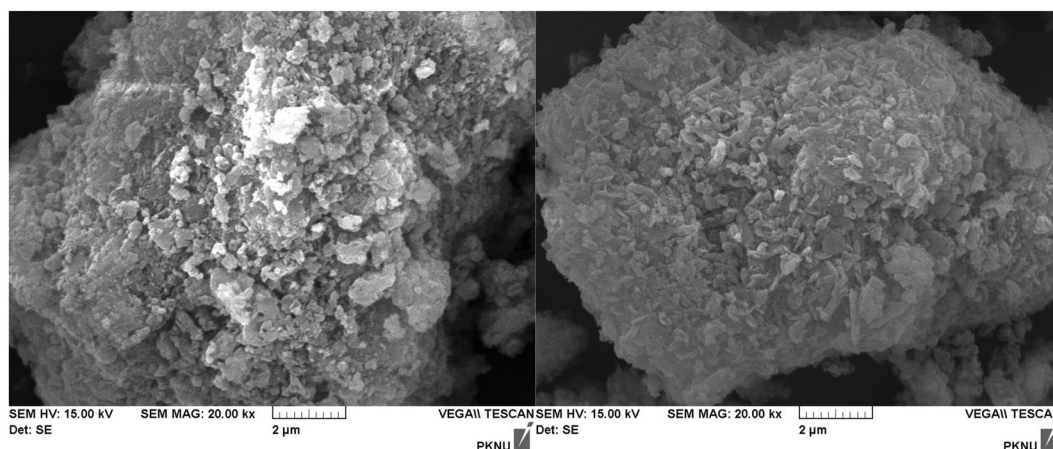


Figure 3. SEM images of the composite mineral adsorbents CMA1 (left) and CMA2 (right).

purposes⁴⁴. The SEM images of CMA1 and CMA2 presented amorphous porous particles, which are consistent with the aggregated forms of albite, calcite, dachiardite, clinoptilolite, and mordenite (Fig. 3). Overall, dachiardite, clinoptilolite, and mordenite can be considered major minerals involved in adsorption for heavy metal control^{45–48}.

Effect of initial pH on Cu, Cd, and Pb ions. The adsorption of heavy metals is significantly influenced by the initial pH of the solution since the initial pH determines the surface charge of the adsorbent and the degree of speciation and ionization of the adsorbate^{49–53}. The effects of the initial pH value were evaluated by the Cu, Cd, and Pb adsorption capacities in the solutions (Fig. 4). The adsorption capacities of Cu in the solutions were determined to be 71–107.5, 126–144.5, and 395.5–479.5 mg/g at initial pH values of 2.78, 4.94, and 6.50, respectively. The adsorption capacities of Cd in the solutions were 261–279, 302–311, and 198–222 mg/g at initial pH values of 2.80, 4.76, and 6.45, respectively. Additionally, the adsorption capacities of Pb in the solutions were determined to be 453.1–495.4, 570.2–594.6, and 613.8–646.5 mg/g at initial pH values of 2.83, 4.98, and 7.01, respectively. At pH < 5.0, Cu²⁺, Cd²⁺, and Pb²⁺ are the primary species in the Cu, Cd, and Pb solutions, respectively; the species vary with solution pH, and the adsorption of Cu, Cd, and Pb ions mainly involves divalent metal ions^{54–56}. Based on the effect of the initial pH on Cu, Cd, and Pb ions, each of adsorption kinetic experiments was conducted at a pH value less than 5.0.

Adsorption kinetic experiments. To determine the equilibrium reaction time, the adsorption of Cu, Cd, and Pb ions on the adsorbents CMA1 and CMA2 were plotted as a function of reaction time in Fig. 5. At the same initial concentration and reaction time, the CMA2 demonstrated better adsorption than the CMA1 (Table 2). The Cu, Cd, and Pb ions adsorption on the CMA1 and CMA2 had almost reached equilibrium within 180 min.

PFO and PSO models were applied to the results of the adsorption kinetic experiments for Cu, Cd, and Pb ions on the adsorbents CMA1 and CMA2. The PFO and PSO models demonstrated different determination coefficient

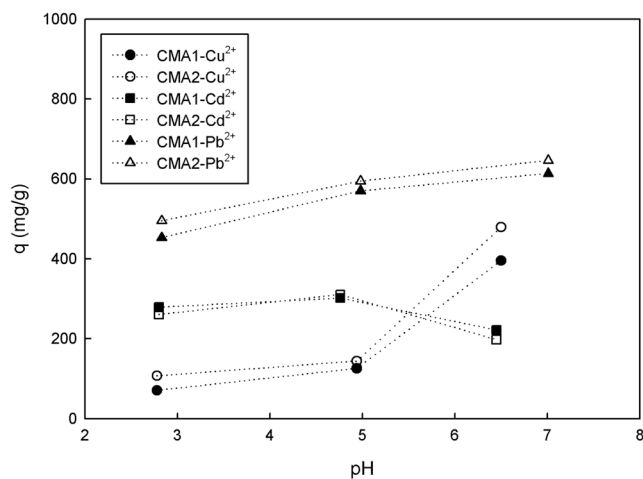


Figure 4. Effect of initial pH on the adsorption capacities of Cu, Cd, and Pb ions.

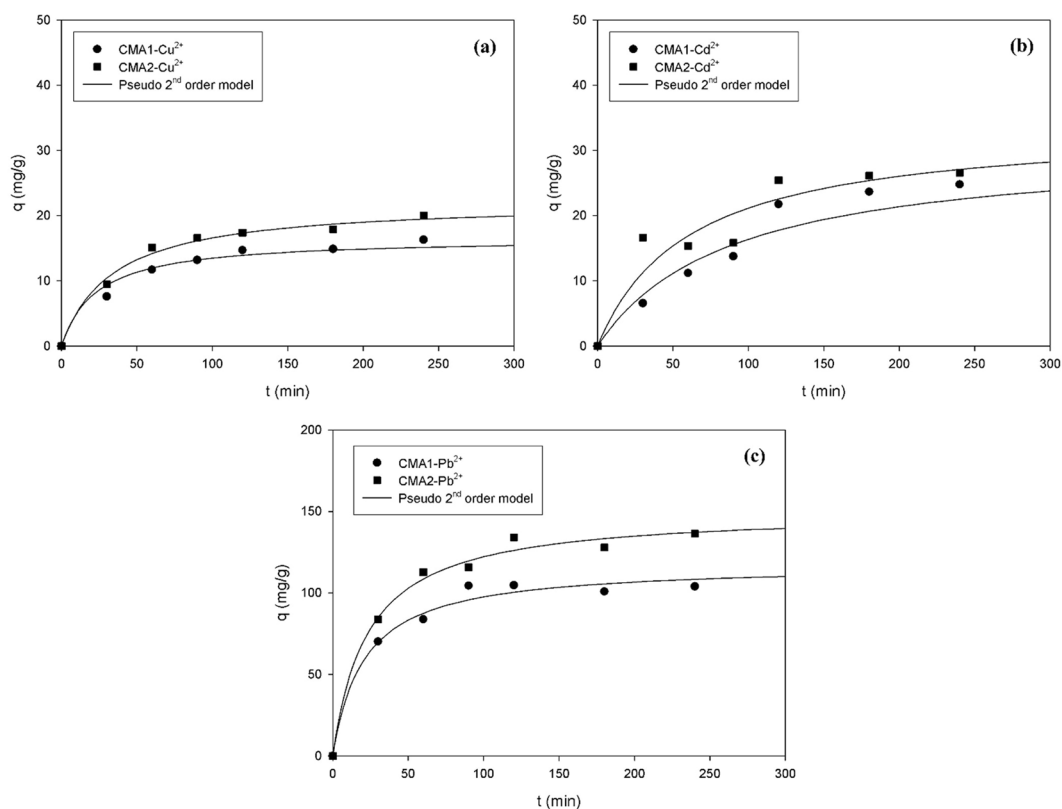


Figure 5. Adsorption kinetics for (a) Cu, (b) Cd, and (c) Pb ions on the adsorbents CMA1 and CMA2.

(r^2) values, between 0.7690–0.9515 and 0.9255–0.9977, respectively, indicating that the latter was more suitable than the former (Fig. 5). The adsorption capacities obtained from the experiments did not agree with the values estimated to reproduce the Cu, Cd, and Pb ions adsorption kinetics with the adsorbents CMA1 and CMA2 from the PFO model. However, the experimental results were similar to the values calculated from the PSO model, and the r^2 values were also very close to unity. Therefore, Cu, Cd, and Pb ions adsorption by the adsorbents CMA1 and CMA2 could be more accurately explained by the PSO model than by the PFO model. Additionally, the adsorbent CMA2 was more effective in removing the heavy metals ions of Pb, Cd, and Cu than the CMA1, in decreasing order of their $q_{e, cal}$ values.

Adsorption isotherm experiments. The adsorption isotherms for Cu, Cd, and Pb ions on the adsorbents CMA1 and CMA2 are plotted in Fig. 6. The isotherm parameters, Q_e , K_L , n , K_F , and r^2 obtained from the Langmuir and Freundlich isotherms are given in Table 3. The results of the adsorption isotherm experiment for

Ions	Adsorbent	C_0 (mgL ⁻¹)	PFO			PSO		
			k_1 (min ⁻¹)	$q_{e,cal}$ (mgg ⁻¹)	r^2	k_2 (gmg ⁻¹ .min ⁻¹)	$q_{e,cal}$ (mgg ⁻¹)	r^2
Cu	CMA1	1000	0.0308	18.2653	0.9515	0.00259	16.6001	0.9900
	CMA2		0.0165	18.4156	0.9040	0.00133	22.2067	0.9971
Cd	CMA1	1000	0.0231	32.5880	0.7690	0.00037	30.7407	0.9255
	CMA2		0.0100	22.6622	0.8529	0.00049	33.8665	0.9604
Pb	CMA1	1000	0.0221	98.4427	0.9416	0.00041	117.6717	0.9950
	CMA2		0.0117	81.0433	0.8143	0.00029	150.4259	0.9977

Table 2. PFO and PSO constants (k_1 , k_2 , and calculated q_e , $q_{e,cal}$) for the adsorption of Cu, Cd, and Pb ions onto the adsorbents CMA1 and CMA2.

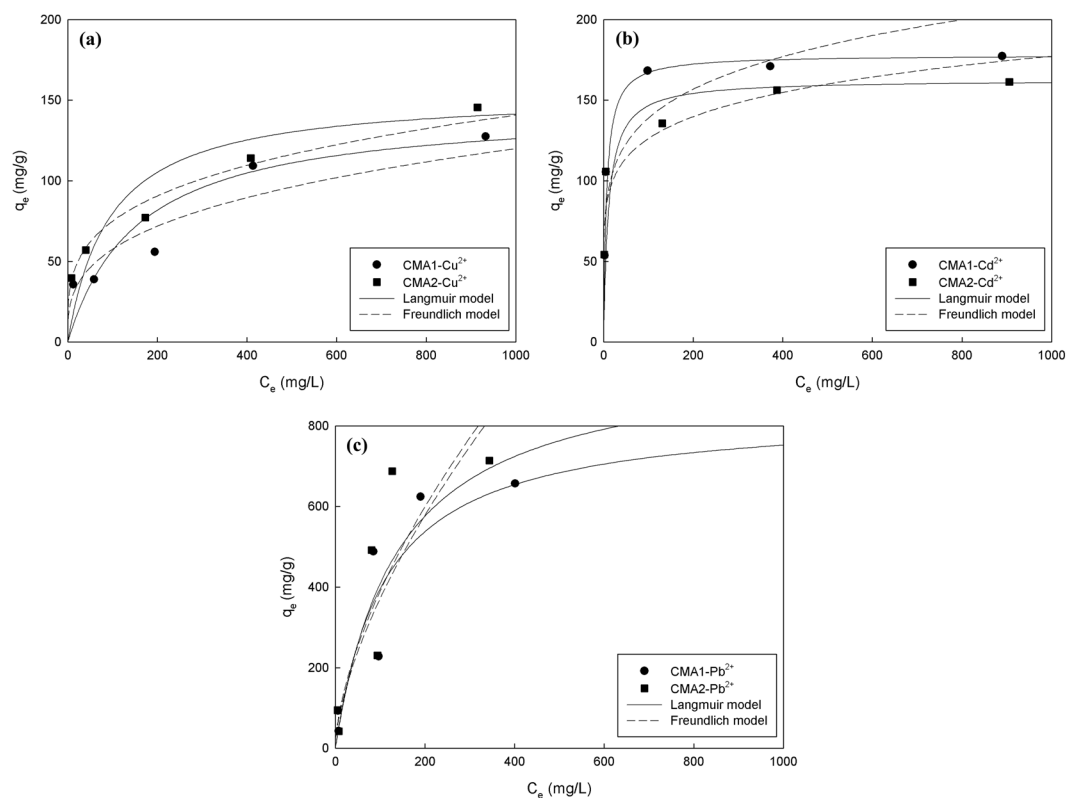


Figure 6. Adsorption isotherms for (a) Cu, (b) Cd, and (c) Pb ions on the adsorbents CMA1 and CMA2.

Cu, Cd, and Pb ions on the adsorbents CMA1 and CMA2 were interpreted by using the Langmuir and Freundlich models. Table 3 and Fig. 6 show that the Langmuir model gave a slightly higher correlation coefficient (r^2) than the Freundlich model, indicating that the two models could both be applied to the heavy metal solutions on a spherical monolayer surface with a weak heterogeneity of the surface. The adsorption capacities of Cu, Cd, and Pb ions by the Langmuir model were 145.84–154.71 mg/g, 162.58–177.99 mg/g, and 802.23–932.08 mg/g, respectively, while the adsorption capacities of Cu and Cd ions by Erdem *et al.*² and Ok *et al.*³ were 9.0–23.3 mg/g using clinoptilolite (natural zeolite) and ZeoAds (a mixture of zeolite and Portland cement).

The maximum adsorption capacities (Q_m) of Cu, Cd, and Pb ions by using the Langmuir model were determined to be 802.23 mg/g (CMA1) and 932.08 mg/g (CMA2) for Pb, 177.99 mg/g (CMA1) and 162.58 mg/g (CMA2) for Cd, and 145.84 mg/g (CMA1) and 154.71 mg/g (CMA2) for Cu, after dosing the adsorbents with only 1 g/L of the heavy metal solution; and hence, these values are significantly higher than those of the existing adsorbents as presented in Table 1. By comparison, an adsorption experiment using a highly porous composite material with immobilization of an organic ligand onto silica monoliths⁵⁷ that was performed to efficiently remove Pb ions in wastewater resulted in a Q_m of 204.34 mg/g, and an adsorption experiment using a mesoporous composite material synthesized by the immobilization of an organic ligand onto mesoporous silica for effectively removing Cu ions in aqueous solution obtained a Q_m of 197.15 mg/g⁵⁸.

Ions	Adsorbents	Langmuir			Freundlich		
		Q_m , mg/g	K_L , L/mg	r^2	K_F , (mg/g) (L/mg) ^{1/n}	n	r^2
Cu	CMA1	145.84	0.0064	0.9346	13.3202	3.1426	0.8617
	CMA2	154.71	0.0107	0.9722	21.3117	3.6593	0.9791
Cd	CMA1	177.99	0.1542	0.9998	61.9791	5.7072	0.8094
	CMA2	162.58	0.0921	0.9993	63.9752	6.7771	0.8261
Pb	CMA1	802.23	0.0132	0.9617	22.7868	1.6284	0.8948
	CMA2	932.08	0.0113	0.8917	22.2813	1.5406	0.8688

Table 3. Calculated maximum adsorption capacity (Q_m) values for Cu, Cd, and Pb ions and parameters of Langmuir and Freundlich models using the adsorbents CMA1 and CMA2.

Discussion and Conclusions

In this study, the adsorption performance and adsorption equilibrium characteristics of the heavy metal ions were evaluated through adsorption isotherm and adsorption kinetic experiments. We applied the composite adsorbents CMA1 (zeolite with clinoptilolite of over 20 weight percent and feldspar of ~10 percent, with Portland cement) and CMA2 (zeolite with feldspar of over 15 weight percent and ~9 percent clinoptilolite, with Portland cement) to heavy metal (Cu, Cd, and Pb ions) solutions.

The adsorption kinetic experiments results showed that the adsorption of the heavy metal ions almost reached within 180 min. PFO and PSO models for Cu, Cd, and Pb ions on the adsorbents CMA1 and CMA2 resulted in different r^2 values of 0.7690–0.9515 and 0.9255–0.9977, respectively, indicating that the PSO model was more suitable than the PFO model. Furthermore, the adsorbent CMA2 was more effective in removing the heavy metal ions of Cu, Cd, and Pb than the CMA1, in decreasing order of their $q_{e\text{ cal}}$ values.

The adsorption isotherm experiments showed that both the Langmuir model and the Freundlich model were applicable to the heavy metal solutions because the adsorbents had spherical monolayer surfaces with a weak heterogeneity of the surface. The maximum adsorption capacities of Cu, Cd, and Pb ions from the Langmuir model resulted were 802.23 mg/g (CMA1) and 932.08 mg/g (CMA2) for Pb, 177.99 mg/g (CMA1) and 162.58 mg/g (CMA2) for Cd, and 145.84 mg/g (CMA1) and 154.71 mg/g (CMA2) for Cu, dosing the adsorbents at only 1 g/L of the heavy metal solution. These maximum adsorption capacities were significantly higher than the maximum adsorption capacities of Cu, Cd, and Pb ions using other adsorbents, as presented in Table 1.

Furthermore, the adsorbent CMA2, including cost-effective natural feldspar, displayed better adsorption capacity than the CMA1. The results of this study can be applied to effectively remove heavy metal ions in contaminated water and wastewater since both adsorbents (CMA1 and CMA2) showed excellent removal efficiency of heavy metal ions in solution. Future research will be focused on revealing the mechanism of the different performances on the heavy metal (Cu, Cd, and Pb) ions by the adsorbents CMA1 and CMA2, which is probably related to the feldspar content.

References

- Garcia-Sanchez, A., Alastuey, A. & Querol, X. Heavy metal adsorption by different minerals: application to the remediation of polluted soils. *Sci. Total Environ.* **242**, 179–188 (1999).
- Erdem, E., Karapinar, N. & Donat, R. The removal of heavy metal cations by natural zeolites. *J Colloid Interface Sci* **280**, 309–314 (2004).
- Ok, Y. S., Yang, J. E., Zhang, Y. S., Kim, S. J. & Chung, D. Y. Heavy metal adsorption by a formulated zeolite-Portland cement mixture. *J. Hazard. Mater.* **147**, 91–96 (2007).
- Park, S. B. & Hwang, J. Adsorption characteristics of altered feldspar porphyry for heavy metals. *Journal of Korean Earth Science Society* **29**, 246–254 (2008).
- Nguyen, T. C. *et al.* Simultaneous adsorption of Cd, Cr, Cu, Pb, and Zn by an iron-coated Australian zeolite in batch and fixed-bed column studies. *Chem Eng J* **270**, 393–404 (2015).
- He, K., Chen, Y., Tang, Z. & Hu, Y. Removal of heavy metal ions from aqueous solution by zeolite synthesized from fly ash. *Environ Sci Pollut Res* **23**, 2778–2788 (2016).
- Taamneh, Y. & Sharadqah, S. The removal of heavy metals from aqueous solution using natural Jordanian zeolite. *Appl Water Sci* **7**, 2021–2028 (2017).
- Lee, C. H., Park, J. M. & Lee, M. G. Competitive adsorption in binary solution with different mole ratio of Sr and Cs by zeolite A: adsorption isotherm and kinetics. *J. Environ. Sci. Int* **24**, 151–162 (2015).
- Klute, A. Physical and mineralogical methods. *Planning* **8**, 79 (1986).
- Jama, M. A. & Yu'cel, H. Equilibrium studies of sodium-ammonium, potassium-ammonium, and calcium-ammonium exchanges on clinoptilolite zeolite. *Sep Sci Technol* **24**, 1393–1416 (1989).
- Zamzow, M. J., Eichbaum, B. R., Sandgren, K. R. & Shanks, D. E. Removal of heavy metals and other cations from wastewater using zeolites. *Sep Sci Technol* **25**, 1555–1569 (1990).
- Mier, M. V., Callejas, R. L., Gehr, R., Cisneros, B. E. J. & Alvarez, P. J. Heavy metal removal with Mexican clinoptilolite: multi-component ionic exchange. *Water Res.* **35**, 373–378 (2001).
- Inglezakis, V. J., Loizidou, M. D. & Grigoropoulou, H. P. Equilibrium and kinetic ion exchange studies of Pb²⁺, Cr³⁺, Fe³⁺ and Cu²⁺ on natural clinoptilolite. *Water Res.* **36**, 2784–2792 (2002).
- Noh, J. H. & Koh, S. M. Mineralogical characteristics and genetic environment of zeolitic bentonite in Yeongil area. *J. Miner. Soc. Korea.* **17**, 135–145 (2004).
- Awual, M. R. *et al.* Copper (II) ions capturing from water using ligand modified a new type mesoporous adsorbent. *Chem Eng J.* **221**, 322–330 (2013a).
- Awual, M. R. *et al.* Trace copper (II) ions detection and removal from water using novel ligand modified composite adsorbent. *Chem Eng J.* **222**, 67–76 (2013b).

17. Awual, M. R. A novel facial composite adsorbent for enhanced copper (II) detection and removal from wastewater. *Chem Eng J.* **266**, 368–375 (2015).
18. Awual, M. R. *et al.* Schiff based ligand containing nano-composite adsorbent for optical copper (II) ions removal from aqueous solutions. *Chem Eng J.* **279**, 639–647 (2015).
19. Awual, M. R. Assessing of lead (III) capturing from contaminated wastewater using ligand doped conjugate adsorbent. *Chem Eng J.* **289**, 65–73 (2016).
20. Awual, M. R., Hasan, M. M., Khaleque, M. A. & Sheikh, M. C. Treatment of copper (II) containing wastewater by a newly developed ligand based facial conjugate materials. *Chem Eng J.* **288**, 368–376 (2016).
21. Awual, M. R. New type mesoporous conjugate material for selective optical copper (II) ions monitoring & removal from polluted waters. *Chem Eng J.* **307**, 85–94 (2017).
22. Awual, M. R. *et al.* Efficient detection and adsorption of cadmium (II) ions using innovative nano-composite materials. *Chem Eng J.* **343**, 118–127 (2018).
23. Shahat, A. *et al.* Large-pore diameter nano-adsorbent and its application for rapid lead (II) detection and removal from aqueous media. *Chem Eng J.* **273**, 286–295 (2015).
24. Conca, J. L. & Wright, J. An Apatite II permeable reactive barrier to remediate groundwater containing Zn, Pb and Cd. *Appl Geochem* **21**, 1288–1300 (2006).
25. Liu, Y., Mou, H., Chen, L., Mirza, Z. A. & Liu, L. Cr (VI)-contaminated groundwater remediation with simulated permeable reactive barrier (PRB) filled with natural pyrite as reactive material: environmental factors and effectiveness. *J. Hazard. Mater.* **298**, 83–90 (2015).
26. Misaelides, P. Application of natural zeolites in environmental remediation: A short review. *Microporous Mesoporous Mater* **144**, 15–18 (2011).
27. Olu-Owolabi, B. I. *et al.* Fractal-like concepts for evaluation of toxic metals adsorption efficiency of feldspar-biomass composites. *J Clean Prod* **171**, 884–891 (2018).
28. Wang, S. & Peng, Y. Natural zeolites as effective adsorbents in water and wastewater treatment. *Chem Eng J.* **156**, 11–24 (2010).
29. Wantanaphong, J., Mooney, S. J. & Bailey, E. H. Natural and waste materials as metal sorbents in permeable reactive barriers (PRBs). *Environ Chem Lett.* **3**, 19–23 (2005).
30. Lagergren, S. Zur theorie der sogenannten adsorption gelöster stoffe, Kungliga Svenska Vetenskapsakademiens. *Handlingar* **24**, 1–39 (1898).
31. Ho, Y. S. & McKay, G. The kinetics of sorption of basic dyes from aqueous solution by sphagnum moss peat. *Can J Chem Eng* **76**, 822–827 (1998).
32. Vanderborght, B. M. & Grieken, R. E. V. Enrichment of trace metals in water by adsorption on activated carbon. *Anal. Chem.* **49**, 311–316 (1977).
33. Langmuir, I. The adsorption of gases on plane surfaces of glass, mica and platinum. *J. Am. Chem. Soc.* **40**, 1361–1403 (1918).
34. Freundlich, H. Kapillarchemie, eine Darstellung der Chemie der Kolloide und verwandter Gebiete (von Dr. Herbert Freundlich, Akademische Verlagsgesellschaft, 1909).
35. Voudrias, E., Fytianos, K. & Bozani, E. Sorption–desorption isotherms of dyes from aqueous solutions and wastewaters with different sorbent materials. *Global Nest Int. J.* **4**, 75–83 (2002).
36. Mohan, S. V. & Karthikeyan, J. Removal of lignin and tannin colour from aqueous solution by adsorption onto activated charcoal. *Environ. Pollut.* **97**, 183–187 (1997).
37. Goldberg, S. Equations and models describing adsorption processes in soils. *Soil Sci Soc Am J* **8**, 489–517 (2005).
38. Rosa, G. *et al.* Recycling poultry feathers for Pb removal from wastewater: kinetic and equilibrium studies. *International Journal of Chemical and Biomolecular Engineering* **1**, 185–193 (2008).
39. Aşçı, Y., Nurbaş, M. & Açikel, Y. S. A comparative study for the sorption of Cd (II) by K-feldspar and sepiolite as soil components, and the recovery of Cd (II) using rhamnolipid biosurfactant. *J. Environ. Manage.* **88**, 383–392 (2008).
40. Ding, D. *et al.* U (VI) ion adsorption thermodynamics and kinetics from aqueous solution onto raw sodium feldspar and acid-activated sodium feldspar. *J Radioanal Nucl Chem* **299**, 1903–1909 (2014).
41. Eba, F. *et al.* Treatment of aqueous solution of lead content by using natural mixture of kaolinite-albite-montmorillonite-illite clay. *Journal of Applied Sciences* **11**, 2536–2545 (2011).
42. Tsitsishvili, G. V., Andronikashvili, T. G., Kirov, G. R. & Filizova, L. D. *Natural Zeolites* (Ellis Horwood, 1992).
43. Inglezakis, V. J. The concept of “capacity” in zeolite ion-exchange systems. *J Colloid Interface Sci* **281**, 68–79 (2005).
44. Perraki, T., Kakali, G. & Kontoleon, F. The effect of natural zeolites on the early hydration of Portland cement. *Microporous Mesoporous Mater* **61**, 205–212 (2003).
45. Huang, C. P. & Hao, O. J. Removal of some heavy metals by mordenite. *Environ Technol* **10**, 863–874 (1989).
46. Rosales-Landeros, C., Barrera-Díaz, C. E., Bilyeu, B., Guerrero, V. V. & Núñez, F. U. A review on Cr (VI) adsorption using inorganic materials. *Am J Analyt Chem* **4**, 8 (2013).
47. Seliman, A. F. & Borai, E. H. Utilization of natural chabazite and mordenite as a reactive barrier for immobilization of hazardous heavy metals. *Environ Sci Pollut Res Int* **18**, 1098–1107 (2011).
48. Wang, X. S. Equilibrium and Kinetic Analysis for Cu²⁺ and Ni²⁺ adsorption onto Na-Mordenite. *The Open Environmental Pollution & Toxicology Journal* **1**, 107–111 (2009).
49. Awual, M. R., Rahman, I. M., Yaita, T., Khaleque, M. A. & Ferdows, M. pH dependent Cu (II) and Pd (II) ions detection and removal from aqueous media by an efficient mesoporous adsorbent. *Chem Eng J.* **236**, 100–109 (2014).
50. Camacho, L. M., Deng, S. & Parra, R. R. Uranium removal from groundwater by natural clinoptilolite zeolite: effects of pH and initial feed concentration. *J. Hazard. Mater.* **175**, 393–398 (2010).
51. Cho, H., Oh, D. & Kim, K. A study on removal characteristics of heavy metals from aqueous solution by fly ash. *J. Hazard. Mater.* **127**, 187–195 (2005).
52. Glatstein, D. A. & Francisca, F. M. Influence of pH and ionic strength on Cd, Cu and Pb removal from water by adsorption in Na-bentonite. *Appl Clay Sci* **118**, 61–67 (2015).
53. Kwon, J. S., Yun, S. T., Lee, J. H., Kim, S. O. & Jo, H. Y. Removal of divalent heavy metals (Cd, Cu, Pb, and Zn) and arsenic (III) from aqueous solutions using scoria: kinetics and equilibria of sorption. *J. Hazard. Mater.* **174**, 307–313 (2010).
54. Kadirvelu, K., Faur-Brasquet, C. & Cloirec, P. L. Removal of Cu(II), Pb(II), and Ni(II) by Adsorption onto Activated Carbon Cloths. *Langmuir* **16**, 8404–8409 (2000).
55. Boparai, H. K., Joseph, M. & O’Carroll, D. M. Cadmium (Cd²⁺) removal by nano zerovalent iron: surface analysis, effects of solution chemistry and surface complexation modeling. *Environ Sci Pollut Res Int* **20**, 6210–6221 (2013).
56. Yang, S. *et al.* Impact of environmental conditions on the sorption behavior of Pb(II) in Na-bentonite suspensions. *J. Hazard. Mater.* **183**, 632–640 (2010).
57. Awual, M. R. Innovative composite material for efficient and highly selective Pb(II) ion capturing from wastewater. *J Mol Liq* **284**, 502–510 (2019).
58. Awual, M. R., Hasan, M. M., Rahman, M. M. & Asiri, A. M. Novel composite material for selective copper(II) detection and removal from aqueous media. *J Mol Liq* **283**, 772–780 (2019).

Acknowledgements

This research was funded by National Research Foundation of Korea (NRF) under the Ministry of Science and ICT (NRF- 2017R1A2B2009033) as well as by the Ministry of Oceans and Fisheries, South Korea as a part of the project titled 'Development on technology for offshore waste final disposal'.

Author Contributions

S.Y.H., W.R.L. and C.H.L. wrote the manuscript; W.R.L., C.H.L. and H.J.P. conducted the experiment using the composite mineral adsorbents; S.W.K., E.K.C., M.H.O. and S.N.S. developed the composite mineral adsorbents.

Additional Information

Competing Interests: The authors declare no competing interests.

Publisher's note Springer Nature remains neutral with regard to jurisdictional claims in published maps and institutional affiliations.



Open Access This article is licensed under a Creative Commons Attribution 4.0 International License, which permits use, sharing, adaptation, distribution and reproduction in any medium or format, as long as you give appropriate credit to the original author(s) and the source, provide a link to the Creative Commons license, and indicate if changes were made. The images or other third party material in this article are included in the article's Creative Commons license, unless indicated otherwise in a credit line to the material. If material is not included in the article's Creative Commons license and your intended use is not permitted by statutory regulation or exceeds the permitted use, you will need to obtain permission directly from the copyright holder. To view a copy of this license, visit <http://creativecommons.org/licenses/by/4.0/>.

© The Author(s) 2019